

# Effect of Nb Doping on Crystalline Orientation, Electric and Fatigue Properties of PZT Thin Films Prepared by Sol-Gel Process

Q. Li, X. Wang, F. Wang, J. Dou, W. Xu, H. Zou\*

Key Laboratory for Micro/Nano Technology and Systems of Liaoning Province, Dalian University of Technology, Dalian 116024, People's Republic of China

received May 8, 2017; received in revised form August 22, 2017; accepted November 6, 2017

## Abstract

Pb(Nb<sub>x</sub>Zr<sub>0.52</sub>Ti<sub>0.48</sub>)O<sub>3</sub> (PNZT) ( $x = 0\%$ ,  $1\%$ ,  $2\%$ ,  $3\%$ ,  $4\%$ ,  $5\%$ ) thin films were prepared in a sol-gel process to investigate the effects of Nb doping on the crystalline orientation, electric and fatigue properties of lead zirconate titanate (PZT) films. X-ray diffraction (XRD) and scanning electron microscope (SEM) analyses showed that PNZT films with Nb doping concentration below  $5\%$  exhibited a dense perovskite structure with (100) preferred orientation. The maximum dielectric constant was obtained in  $4\%$  Nb-doped PZT film with a precision impedance analyzer. Remnant polarization and fatigue resistance were enhanced significantly with  $2\%$  Nb dopant.

**Keywords:** PNZT thin films, (100) preferred orientation, microstructure, fatigue resistance, sol-gel process

## I. Introduction

PZT thin films have been extensively studied owing to their excellent dielectric, ferroelectric and piezoelectric properties, which has made various applications such as random access memory, ferroelectric capacitors and micro-electro-mechanical systems (MEMS) possible in recent years<sup>1–4</sup>. The common methods for fabricating PZT thin films are sputtering, metal-organic chemical vapor deposition, chemical solution deposition, pulsed laser ablation deposition and the sol-gel process<sup>5–9</sup>. Among these, the sol-gel process has aroused popular interest because of its precise composition control, low-temperature processing, low cost of fabrication and ease of doping modification.

It is widely accepted that the properties of PZT films depend strongly on many parameters, including stoichiometric composition, sintering conditions, preferred orientation and doping<sup>7, 10, 11</sup>. Some researchers have indicated that the piezoelectric response of (100)-oriented PZT films in the vicinity of morphotropic phase boundary composition could be greatly enhanced<sup>12, 13</sup>. In addition, PZT thin films suffer significant ferroelectric fatigue when subject to repeated polarization switching because of the long-range migration of space charge. In order to obtain (100)-oriented PZT thin films and resolve the fatigue problem, many efforts have been focused on introducing a seed layer to induce the growth of PZT films, such as LaNiO<sub>3</sub>, PbTiO<sub>3</sub> and PbO seed layers<sup>9, 14, 15</sup>. However, introducing a seed layer leads to an increase in process costs and a longer fabrication time.

Doping is often used to enhance the properties of PZT thin films. Many researchers have done a great quantity

of work to evaluate the electric properties and fatigue resistance of PZT films doped with La, Gd, Nd, Nb, Mn, etc.<sup>9, 16–19</sup>. Donor doping is one effective way to prevent the formation of oxygen vacancies due to charge compensation. In particular, niobium additive is considered as donor dopant to improve the dielectric, ferroelectric and piezoelectric properties of PZT films. Zhang<sup>9</sup> *et al.* fabricated (100)-oriented PNZT films by introducing a Pb-TiO<sub>3</sub> seed layer prepared by means of chemical solution deposition. Pintea<sup>20</sup> and Thakur<sup>21</sup> investigated the effect of Nb doping on the grain size, dielectric and ferroelectric properties of PZT ceramics. Nevertheless, there has been only few studies discussing the effect of Nb doping on the fatigue resistance of PZT films. Furthermore, preparing (100)-oriented PNZT thin films on Pt(111)/Ti/SiO<sub>2</sub>/Si(100) substrates remains a challenge.

In this paper, Nb-doped PZT thin films with the concentration of  $0\%$ ,  $1\%$ ,  $2\%$ ,  $3\%$ ,  $4\%$  and  $5\%$  were deposited on Pt(111)/Ti/SiO<sub>2</sub>/Si(100) substrates by means of the sol-gel process. (100)-oriented PNZT thin films with excellent fatigue resistance were obtained by using conventional furnace heat process and appropriate doping concentration. Simultaneously, the effects of Nb doping on crystalline orientation, microstructure, dielectric, ferroelectric properties and fatigue resistance of PZT thin films were investigated.

## II. Experiments

The PNZT precursor solutions were prepared with nominal compositions of Pb(Nb<sub>x</sub>Zr<sub>0.52</sub>Ti<sub>0.48</sub>)O<sub>3</sub> ( $x = 0\%$ ,  $1\%$ ,  $2\%$ ,  $3\%$ ,  $4\%$ ,  $5\%$ ). The raw materials used for preparing the precursors were lead acetate trihydrate ((Pb(CH<sub>3</sub>COO)<sub>2</sub>·3H<sub>2</sub>O), zirconium nitrate (Zr(NO<sub>3</sub>)<sub>4</sub>·5H<sub>2</sub>O), tetrabutyl titanate (C<sub>16</sub>H<sub>36</sub>O<sub>4</sub>Ti) and niobium ethoxide (Nb(C<sub>2</sub>H<sub>5</sub>O)<sub>5</sub>). 2-methoxyethanol (C<sub>3</sub>H<sub>8</sub>O<sub>2</sub>)

\* Corresponding author: [zouhl@dlut.edu.cn](mailto:zouhl@dlut.edu.cn)

was selected as the solvent and acetylacetone ( $\text{C}_5\text{H}_8\text{O}_2$ ) as the chelating agent. The lead acetate trihydrate, zirconium nitrate, tetrabutyl titanate, niobium ethoxide and acetylacetone were dissolved in 2-methoxyethanol and refluxed for 24 h. 20 % excess lead was used to compensate for the lead loss during the sintering process. Formamide ( $\text{CH}_3\text{NO}$ ) was selected to prevent cracks and acetic acid ( $\text{C}_2\text{H}_4\text{O}_2$ ) to adjust the pH. The ratio of Zr/Ti was kept at 52/48 and the concentration of precursor solutions was at 0.33 M. Before being used for coating, the PNZT precursor solutions were filtered through syringe filters of 0.22  $\mu\text{m}$  pore size.

The filtered PNZT precursor solutions were spin-coated on Pt(111)/Ti/SiO<sub>2</sub>/Si(100) substrates at 800 rpm for 9 s and 3000 rpm for 30 s. The films were dried at 150 °C for 5 min to eliminate moisture, pyrolyzed at 450 °C for 5 min to remove the organics, and then annealed at 600 °C for 10 min to induce complete crystallization. The above-mentioned steps were repeated 16 times to obtain about 1- $\mu\text{m}$ -thick PNZT thin films. And then the Pt top electrodes were sputtered onto the PNZT films. The top electrodes, bottom electrode and PCB circuit board are connected by means of gold wire welded with silver paste.

The crystalline structure and preferential orientation of the PNZT thin films were analyzed with an X-ray diffractometer (D8 Bruker, Bruker, Germany) with  $\text{CuK}\alpha$  radiation in a wide range of Bragg angle ( $20^\circ \leq 2\theta \leq 60^\circ$ ) at room temperature. In order to evaluate the degree of the (100)

preferred orientation, the volume fraction  $a$  is calculated using the following equation 22:

$$\alpha = \frac{I_{(100)}}{I_{(100)} + I_{(110)} + I_{(111)}} \times 100\% \quad (1)$$

where  $I_{(100)}$ ,  $I_{(110)}$  and  $I_{(111)}$  are the diffraction intensities of (100), (110) and (111) peaks, respectively. The microstructure of PNZT films was observed with a scanning electron microscope (S-4800, Hitachi, Japan). The dielectric constant of the films was obtained using a precision impedance analyzer (4294A, Agilent Technologies, US), as a function of frequencies varying from 0.1 to 100 kHz at ambient temperature. The P-E hysteresis loops and fatigue resistance were characterized by means of a modified Sawyer-Tower circuit.

### III. Results and Discussion

#### (1) The orientation and microstructures

Fig. 1 shows the XRD patterns of undoped and Nb-doped PZT thin films with different Nb doping concentration. It can be noted that all films are completely crystallized in polycrystal perovskite and scarcely any pyrochlore phase is observed. The crystal structure of the PNZT thin films is closely related with the doping concentration. When the concentration of Nb dopant is below 5 %, the PNZT films exhibit combined orientations of the (100), (110) and (111) directions, in which the (100) orientation is the dominant growth

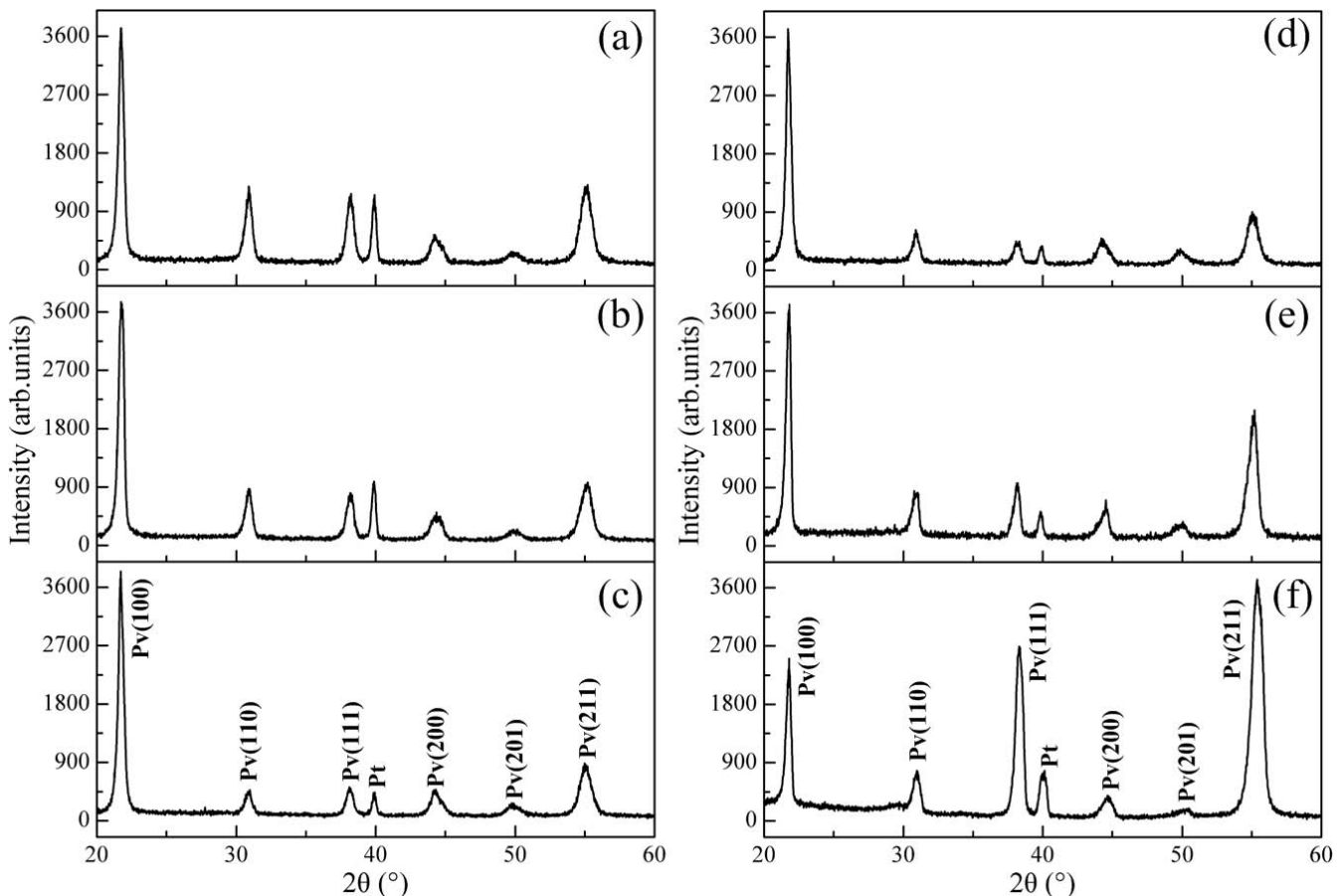


Fig. 1: XRD patterns of (a) undoped, (b) 1 % Nb-doped, (c) 2 % Nb-doped, (d) 3 % Nb-doped, (e) 4 % Nb-doped and (f) 5 % Nb-doped PZT thin films.

direction. After the Nb doping concentration had been increased to more than 2 %, (110), (111), (200), (201) and (211) orientation diffraction peaks increased while (100) orientation diffraction peak gradually weakened. 5 % Nb-doped PZT films are presented with random crystalline orientation and the (211) orientation dominates crystal growth orientation.

Fig. 2 shows the (100) preferential orientation degree ( $a$ ) as a function of Nb doping concentration. It can be seen that the degree of (100) preferred orientation first increases and then decreases as the Nb doping concentration increases from 0 % to 5 %. The maximum (100) preferred orientation degree (80.3 %) is obtained in 2 % Nb-doped PZT film, an increase of 34.3 % compared with the undoped PZT film. The degree slightly decreases to 77.6 % at the doping concentration of 3 %. As the Nb doping concentration increases to 5 %, the  $a$  value is reduced to 42.1 %.

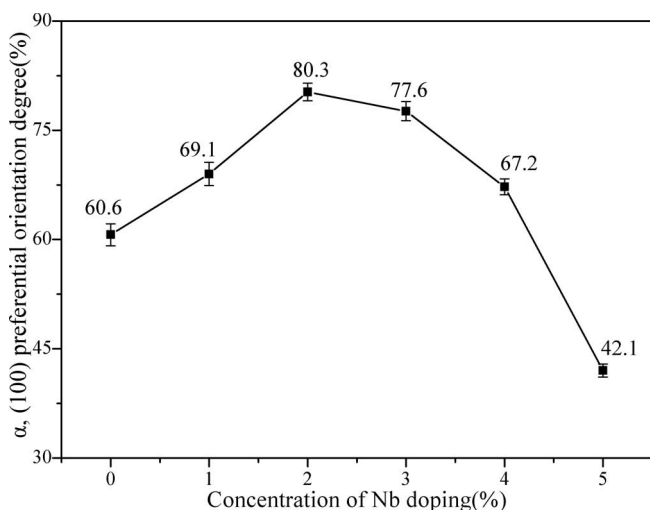


Fig. 2: The (100) preferential orientation degree ( $a$ ) of PNZT thin films as a function of Nb doping concentration.

It is well known that (100) preferred orientation is dependent on the natural growth of the perovskite structure. The (100) crystal orientation has the lowest interfacial energy at crystallization temperature, which makes the (100) oriented nuclei grow more rapidly than other

orientations and then inhibits the growth of other crystal orientations<sup>23</sup>. Besides, there is a positive effect on the (100)-oriented crystal growth of PNZT films under low Nb doping concentration. Therefore, the lowest interface energy and the positive effect of Nb dopant dominate the preferred texture of the PZT films. The ionic radius of  $Zr^{4+}$ ,  $Ti^{4+}$  and  $Nb^{5+}$  in the octahedral coordination are 0.072, 0.0605 and 0.064 nm, respectively. Therefore, the Nb dopant acted as donor dopant and occupied the Zr or Ti position because of the similarity in ionic radii, which generated additional positive charge. To maintain charge neutrality, lead vacancies were then created. When the Nb doping concentration was relatively high, on the one hand, the generation of excessive lead vacancies resulted in PbO accumulation at the grain boundaries, which impeded grain growth<sup>24</sup>. On the other hand, the further addition of Nb ions would aggregate near the grain boundaries and inhibit grain growth<sup>19</sup>. Thus, the (100) preferential orientation degree decreased and the film displayed random crystalline orientation.

The surface and cross-section SEM images of PNZT thin films with different Nb doping concentration are shown in Fig. 3 and Fig. 4. When the doping concentration is less than 5 %, all the films reveal no cracks, distinct grain boundaries (as shown in Fig. 3) and dense columnar microstructure (as shown in Fig. 4(a)–(e)). As the Nb doping concentration increases to 5 %, the PNZT film is presented with an unclear grain boundary, which may be due to the non-dense perovskite structure of the film (as shown in Fig. 4(f)). In addition, the grain size of 4 % Nb-doped PZT film is found to be larger than that of the other films.

## (2) Dielectric and ferroelectric properties

Fig. 5 shows the dielectric constant of PNZT thin films with different Nb doping concentration as a function of frequency ranging from 0.1 to 100 kHz at room temperature. It can be observed that the dielectric constant of all the films decreases as the frequency increases. At lower frequencies, the higher value of the dielectric constant is due to simultaneous presence of all types of polarizations like electronic, ionic and space charges polarization. But at higher frequencies, some polarizations become ineffective and only electronic polarization works<sup>25</sup>.

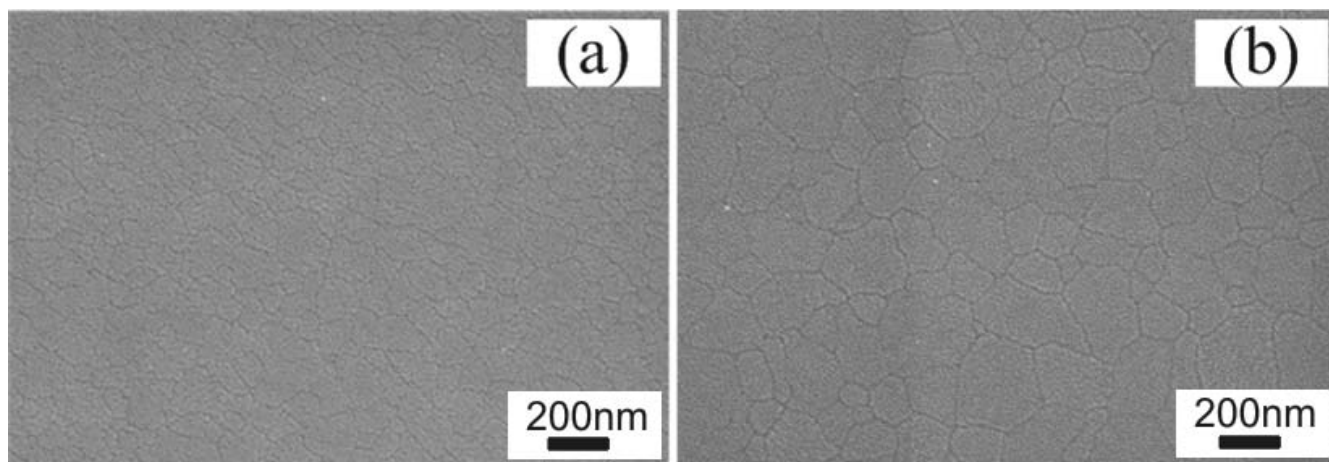


Fig. 3: The surface SEM images of (a) undoped, (b) 4 % Nb-doped PZT thin films.

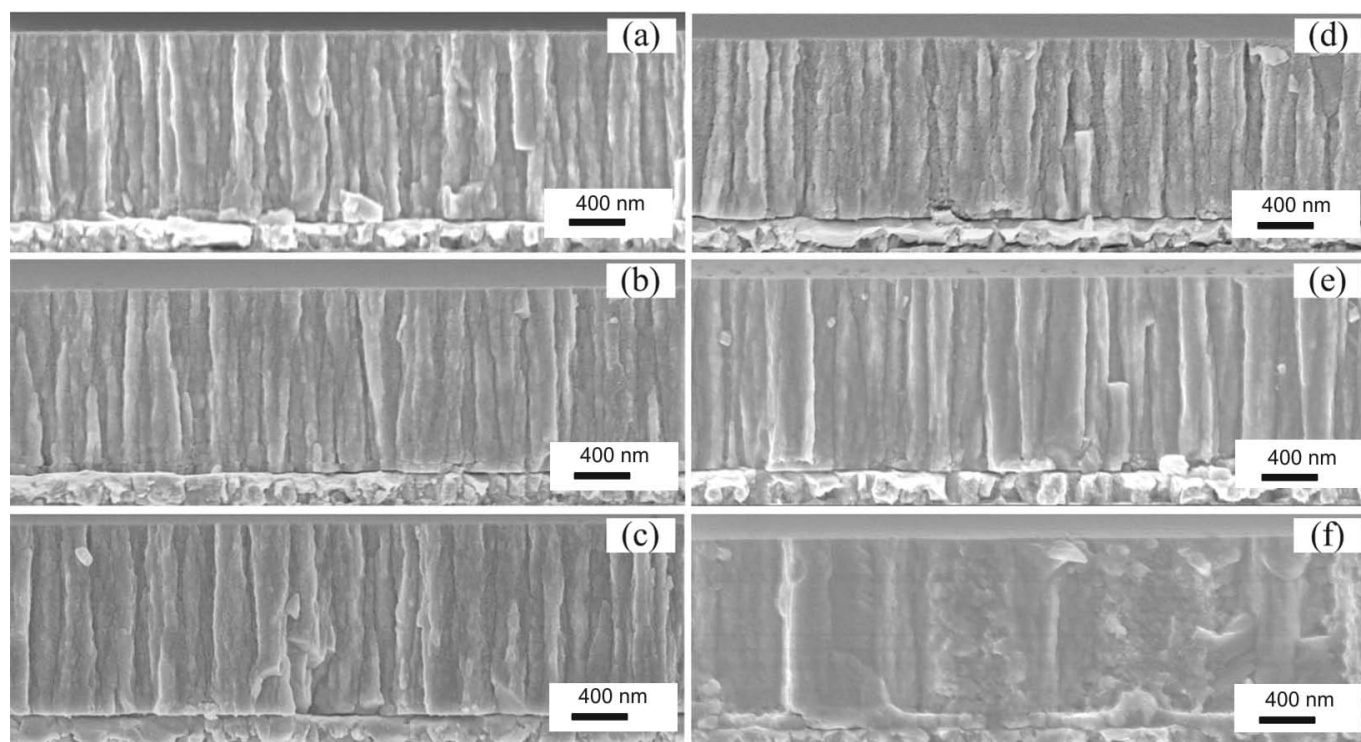


Fig. 4: The cross-section SEM images of (a) undoped, (b) 1 % Nb-doped, (c) 2 % Nb-doped, (d) 3 % Nb-doped, (e) 4 % Nb-doped and (f) 5 % Nb-doped PZT thin films.

In addition, there is a dramatic increase in the dielectric constant with the doping of niobium ions in the PZT perovskite structure. As the Nb doping concentration increases, the dielectric constant first increases and then decreases. The maximum dielectric constant is obtained in 4 % Nb-doped PZT film, reaching 1412.5 at 100 Hz, an increase of 46.9 % compared with undoped PZT films. Because niobium mainly substituted for the  $Zr^{4+}$  or  $Ti^{4+}$  ions, lead vacancies were created to maintain charge neutrality. The lead vacancies could reduce local stresses in the lattice, which in turn promoted the mobility of domain walls and accounted for the improved dielectric properties<sup>19</sup>. As the Nb doping concentration increased to 5 %, on the one hand, excess Nb dopant segregated at the grain boundaries and prohibited grain growth, thus reducing the domain wall motion. On the other hand, the formation of PbO owing to excessive lead vacancies assembled at the grain boundaries weakened the movement of domain wall. Furthermore, the formation of impurity phases and the presence of non-dense perovskite structure, possible pyrochlore phase, decreased the dielectric constant of the film.

The ferroelectric properties of PNZT thin films are plotted in Fig. 6 and Fig. 7. Fig. 6 shows the P-E hysteresis loops of undoped, 2 % Nb-doped and 5 % Nb-doped PZT thin films at ambient temperature. As can be seen, all films show well-saturated polarization hysteresis loops, while the asymmetries on both polarization and electric field axes appear in the undoped PZT film. It was reported that the space charge accumulation at electrode-ferroelectric interface was considered as the major reason for the polarization asymmetry, while the electric field asymmetry could be associated with the presence of internal electric field<sup>26</sup>. We speculate that the improvement of asymmetric

behavior with the doping of niobium ions in the PZT films is due to a modification of the internal electric field.

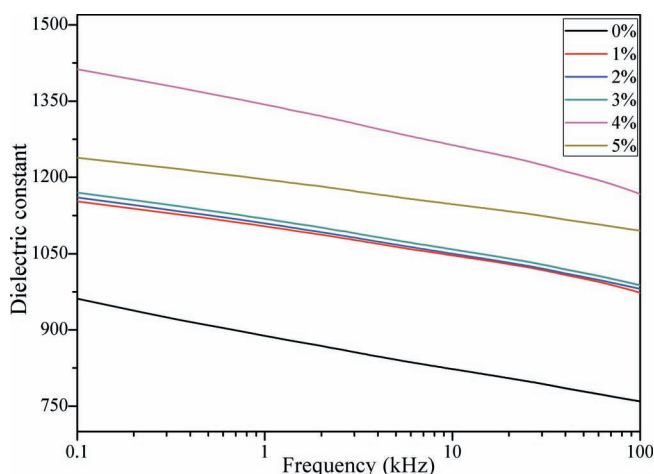


Fig. 5: The dielectric constant of PNZT thin films with different Nb doping concentration as a function of frequency.

Fig. 7 shows the remnant polarization and coercive field of PNZT thin films as a function of Nb doping concentration at 1 kHz. As the niobium dopant percentage continuously increases, the remnant polarization of PNZT films increases and then decreases, while the coercive field decreases and then increases. The maximum value of remnant polarization is produced in 2 % Nb-doped PZT thin film and the lowest value of coercive field is generated in 3 % Nb-doped PZT film. When the Nb doping concentration was relatively low, oxygen vacancies induced domain wall pinning and limited domain wall motion. In contrast, lead vacancies, to maintain charge neutrality, could facilitate the motion of domain walls. The concentration of oxy-



gen vacancy was lower in the PNZT films, so lead vacancies determined the domain wall mobility and improved the ferroelectric properties<sup>19</sup>. When the concentration of Nb doping was increased to more than 3 %, first, excessive Nb dopant gathered at the grain boundary and resulted in lower levels of domain wall motion. Second, there was the development of residual stress in the PNZT films, which could act as energy barrier and impede the domain wall from moving swiftly<sup>27</sup>. Third, a higher amount of niobium led to excessive lead vacancies, which resulted in PbO gathering at the grain boundaries and inhibiting the movement of the domain wall. Thus, these three mechanisms reduced the ferroelectric properties of PNZT thin films.

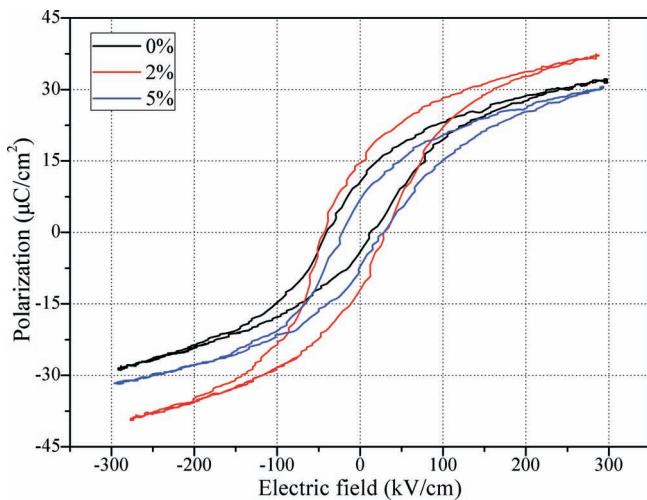


Fig. 6: P-E hysteresis loops of undoped, 2 % Nb-doped and 5 % Nb-doped PZT thin films.

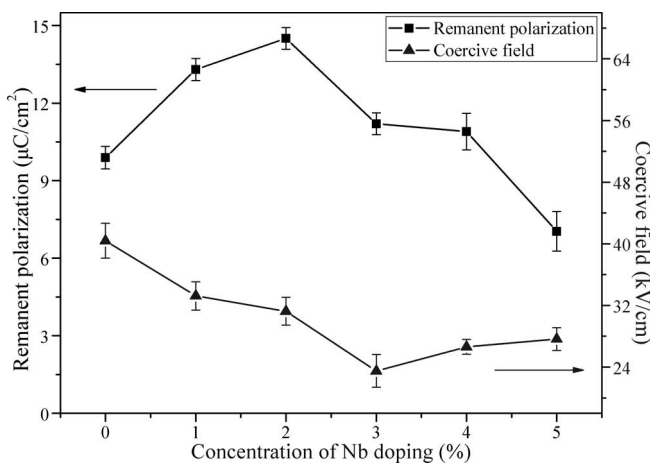


Fig. 7: The ferroelectric properties of PNZT thin films as a function of Nb doping concentration.

### (3) Fatigue resistance

The fatigue resistance of undoped and 2 % Nb-doped PZT thin films as a function of the cycle number is shown in Fig. 8. Fatigue behaviors caused by polarization switching were tested at 10 kHz with bipolar sine wave amplitude of  $\pm 20$  V. As can be seen, there is no evident polarization switching loss in any of the films below  $10^6$  switching cycles, which indicates all films exhibit good fatigue endurance. The fatigue test shows the typical decrease in

remnant polarization, but the fatigue resistance of 2 % Nb-doped PZT film is clearly improved compared with undoped PZT film. After  $10^8$  cycles, the remnant polarization of 2 % Nb-doped PZT thin film decreases to 88 % of its initial value, while that of undoped PZT film decreases to 57 % after  $10^7$  cycles. It is notable that the results of this paper are quite comparable to the results reported by other researchers. Griswold<sup>28</sup> *et al.* reported that Nb doping could improve the fatigue resistance of undoped PZT thin films prepared by means of the dc magnetron-sputtering technique, and the remnant polarization of PNZT films dropped by 20 % after  $10^8$  cycles. Ryder<sup>24</sup> *et al.* found that Nb doping did not have any observable effect on the fatigue resistance of sol-gel-derived PZT films.

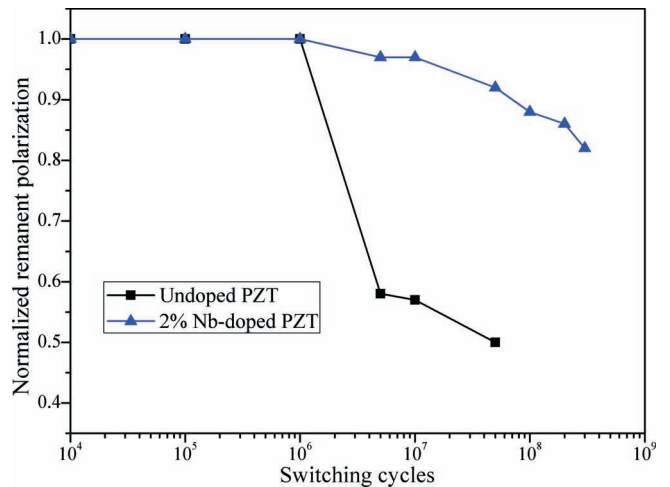


Fig. 8: The fatigue behaviors of undoped and 2 % Nb-doped PZT thin films.

The fatigue resistance of PZT thin films can be improved by doping niobium ions, which may be attributed to the following several factors. First, Nb doping was an effective way to prevent oxygen ions separating from perovskite structure, thus the accumulation of space charge associated with oxygen vacancies at Pt/PZT interface was alleviated, which was usually believed to play a dominant role in the fatigue phenomenon<sup>29</sup>. Second, the introduction of niobium ions in PZT films induced a modification of the internal electric field, which had a great effect on electromigration of charged defects<sup>30</sup>. Third, additional lead vacancies were created to maintain charge neutrality in PNZT films, which could facilitate the domain wall motion and accounted for the improved fatigue resistance<sup>19</sup>.

## IV. Conclusions

The PNZT thin films with Nb doping concentration of 0 %, 1 %, 2 %, 3 %, 4 % and 5 % were fabricated on Pt(111)/Ti/SiO<sub>2</sub>/Si(100) substrates in a sol-gel process. Simultaneously, the effects of Nb doping on crystalline orientation, electric properties and fatigue resistance of PZT films were investigated. When the Nb doping concentration was below 5 %, the PNZT films exhibited (100) preferred orientation with distinct grain boundaries. The maximum dielectric constant of 1412.8 at 100 Hz was obtained in 4 % Nb-doped PZT film, an increase of 46.9 % compared with undoped films. The maximum remnant

polarization is produced at 2 % Nb dopant and the lowest coercive field is generated at 3 % dopant. The fatigue resistance was clearly improved in 2 % Nb-doped PZT film. It is expected that PNZT thin films with highly (100) preferred orientation and enhanced fatigue resistance can be widely utilized in piezoelectric devices, such as piezoelectric inkjet printheads and piezoelectric actuators.

### Acknowledgements

This paper was supported by Zhuhai Seine Technology Co. Ltd, China.

### References

- Bretos, I., Jimenez, R., Wu, A., Kingon, A.I., Vilarinho, P.M., Lourdes, C.M.: Activated Solutions Enabling Low-Temperature Processing of Functional Ferroelectric Oxides for Flexible Electronics, *Adv. Mater.*, **26**, 1405–1409, (2014).
- Tommasi, A., Coletta, G., Balma, D., Marasso, S.L., Perrone, D., Canavese, G., Stassi, S., Bianco, S., Cocuzza, M., Pirri, C.F.: Process optimisation of a MEMS based PZT actuated microswitch, *Microelectron. Eng.*, **119**, 137–140, (2014).
- Byung-Hun, K., Hwa-Sun, L., Sung-Wook, K., Piljoong, K., Yoon-Sok, P.: Hydrodynamic responses of a piezoelectric driven MEMS inkjet print-head, *Sensor. Actuat. A*, **210**, 131–140, (2014).
- Fujii, T., Hishinuma, Y., Mita, T., Naono, T.: Characterization of Nb-doped  $\text{Pb}(\text{Zr,Ti})\text{O}_3$  films deposited on stainless steel and silicon substrates by RF-magnetron sputtering for MEMS applications, *Sensor. Actuat. A*, **163**, 220–225, (2010).
- Maurya, K.K., Halder, S.K., Sen, S., Bose, A., Bysakh, S.: High resolution X-ray and electron microscopy characterization of PZT thin films prepared by RF magnetron sputtering, *Appl. Surf. Sci.*, **313**, 196–206, (2014).
- Veith, M., Bender, M., Lehnert, T., Zimmer, M., Jakob, A.: Novel single-source precursors for the fabrication of  $\text{PbTiO}_3$ ,  $\text{PbZrO}_3$  and  $\text{Pb}(\text{Zr}_{1-x}\text{Ti}_x)\text{O}_3$  thin-films by chemical vapor deposition, *Dalton T.*, **40**, 1175–1182, (2011).
- Nazeer, H., Nguyen, M.D., Sukas, O.S., Rijnders, G., Abelman, L., Elwenspoek, M.C.: Compositional dependence of the young's modulus and piezoelectric coefficient of (110)-oriented pulsed laser deposited pzt thin films, *J. Microelectromech. Syst.*, **24**, 166–173, (2015).
- Chen, Z., Yang, C.T., Li, B., Sun, M.X., Yang, B.C.: Preferred orientation controlling of PZT (52–48) thin films prepared by sol-gel process, *J. Cryst. Growth*, **285**, 627–632, (2005).
- Zhong, J., Kotru, S., Han, H., Jackson, J., Pandey, R.K.: Effect of Nb Doping on Highly {100}-Textured PZT Films Grown on CSD-Prepared  $\text{PbTiO}_3$  Seed Layers, *Int. Ferroelectr.*, **130**, 1–11, (2011).
- Wu, Z., Zhou, J., Chen, W., Shen, J., Yang, H., Zhang, S., Liu, Y.: Improvement in temperature dependence and dielectric tunability properties of  $\text{PbZr}_{0.52}\text{Ti}_{0.48}\text{O}_3$  thin films using  $\text{Ba}(\text{Mg}_{1/3}\text{Ta}_{2/3})\text{O}_3$  buffer layer, *Appl. Surf. Sci.*, **388**, 579–583, (2016).
- Anil, A., Vani, K., Kumar, V.: Influence of defect structure on ferroelectric aging in donor-acceptor hybrid-doped PZT, *Appl. Phys. A*, **122**, 581, 2016.
- Du, X.H., Zheng, J.H., Belegundu, U., Uchino, K.: Crystal orientation dependence of piezoelectric properties of lead zirconate titanate near the morphotropic phase boundary, *Appl. Phys. Lett.*, **72**, 2421–2423, (1998).
- Guo, R., Cross, L.E., Park, S.E., Noheda, B., Cox, D.E., Shirane, G.: Origin of the high piezoelectric response in  $\text{PbZr}_{1-x}\text{Ti}_x\text{O}_3$ , *Phys. Rev. Lett.*, **84**, 5423–5426, (2000).
- Chen, M.S., Wu, T.B., Wu, J.M.: Effect of textured  $\text{LaNiO}_3$  electrode on the fatigue improvement of  $\text{Pb}(\text{Zr}_{0.53}\text{Ti}_{0.47})\text{O}_3$  thin films, *Appl. Phys. Lett.*, **68**, 1430–1432, (1996).
- Gong, W., Li, J.F., Chu, X.C., Gui, Z.L., Li, L.T.: Preparation and characterization of sol-gel derived (100)-textured  $\text{Pb}(\text{Zr,Ti})\text{O}_3$  thin films: PbO seeding role in the formation of preferential orientation, *Acta Mater.*, **52**, 2787–2793, (2004).
- Sheng, T., Narayanan, M., Beihai, M., Shanshan, L., Koritala, R.E., Balachandran, U., Donglu, S.: Effect of lanthanum content and substrate strain on structural and electrical properties of lead lanthanum zirconate titanate thin films, *Mater. Chem. Phys.*, **140**, 427–430, (2013).
- Sun, Q., Wei, Z.D., Wang, F.P., Jiang, Z.H.: Effect of Gd doping on dielectric properties and polarization behavior of lead zirconate titanate thin films, *J. Inorg. Mater.*, **23**, 872–876, (2008).
- Kour, P., Pradhan, S.K., Kumar, P., Sinha, S.K., Kar, M.: Enhanced ferroelectric and piezoelectric properties of  $\text{Nd}^{3+}$  doped PZT nanoceramics. In: International Conference on Condensed Matter and Applied Physics, London, 2016.
- Sun, H.J., Zhang, Y., Liu, X.F., Guo, S.S., Liu, Y., Chen, W.: The effect of Mn/Nb doping on dielectric and ferroelectric properties of PZT thin films prepared by sol-gel process, *J. Sol-Gel Sci. Technol.*, **74**, 378–386, (2015).
- Pintea, J., Dumitru, A., Sbarcea, G., Velciu, G.: Electrical properties of lead titanate zirconate ceramics doped with niobium, *J. Opt. Optoelectron. Adv. Eng. Mater.*, **15**, 99–102, (2013).
- Thakur, O.P., Prakash, C.: Structural and electrical properties of Nb5+ substituted PZT ceramics, *Mod. Phys. Lett. B*, **19**, 1783–1791, (2005).
- Xin, H., Ren, W., Wu, X.Q., Shi, P.: Effect of Mn doping on structures and properties of chemical solution deposited lead zirconate titanate thick films with (100) preferential orientation, *J. Appl. Phys.*, **114**, 027017, (2013).
- Liu, Y.M., Phule, P.P.: Sequence of phase formation in chemically derived ferroelectric lead zirconate titanate  $\text{Pb}(\text{Zr}_{0.4}\text{Ti}_{0.6})\text{O}_3$  thin films, *J. Am. Ceram. Soc.*, **80**, 2410–2412, (1997).
- Ryder, D.F., Raman, N.K.: Sol-gel processing of Nb-doped  $\text{Pb}(\text{Zr,Ti})\text{O}_3$  thin films for ferroelectric memory applications, *J. Electron. Mater.*, **21**, 971–975, (1992).
- Kumar, P., Singh, P., Singh, S., Juneja, J.K., Prakash, C., Raina, K.K.: Influence of lanthanum substitution on dielectric properties of modified lead zirconate titanates, *Ceram. Int.*, **41**, 5177–5181, (2015).
- Rodrigues, S.A.S., Silva, J.P.B., Khodorov, A., Martín-Sánchez, J., Pereira, M., Gomes, M.J.M.: Improvement of the fatigue and the ferroelectric properties of PZT films through a LSCO seed layer, *Mater. Sci. Eng. B*, **178**, 1224–1229, (2013).
- Shakeri, A., Abdizadeh, H., Golobostanfard, M.R.: Fabrication of Nb-doped lead zirconate titanate thick films synthesized by sol-gel dip coating method, *J. Mater. Sci. - Mater. Electron.*, **27**, 5654–5664, (2016).
- Griswold, E.M., Sayer, M., Amm, D.T., Calder, I.D.: The influence of Niobium-doping on lead zirconate titanate ferroelectric thin films, *Can. J. Phys.*, **69**, 260–264, (1991).
- Zhou, L.J., Rixecker, G., Aldinger, F.: Bipolar electric fatigue in ferroelectric Nb-doped PZST ceramics, *Key Eng. Mater.*, **336–338**, 359–362, (2007).
- Yang, J.K., Kim, W.S., Park, H.H.: Enhanced fatigue property through the control of interfacial layer in Pt/PZT/Pt structure, *Jpn. J. Appl. Phys. Part 1*, **39**, 7000–7002, (2000).